Journal of
Mechanics of
Materials and Structures

THIRD-ORDER SHEAR DEFORMATION THEORY FOR STRESS ANALYSIS OF A THICK CONICAL SHELL UNDER PRESSURE

Hamid Reza Eipakchi

Volume 5, Nº 1 January 2010

mathematical sciences publishers

JOURNAL OF MECHANICS OF MATERIALS AND STRUCTURES
Vol. 5, No. 1, 2010

THIRD-ORDER SHEAR DEFORMATION THEORY FOR STRESS ANALYSIS OF A THICK CONICAL SHELL UNDER PRESSURE

HAMID REZA EIPAKCHI

The stresses and displacements of a thick conical shell with varying thickness under nonuniform internal pressure have been calculated analytically using third-order shear deformation theory. The governing equations, which are a system of differential equations with variable coefficients, have been solved analytically with the matched asymptotic expansion of the perturbation theory. The effects of higher-order approximations on the radial and axial displacements, von Mises stress, and shear stress have been studied. The results have been compared with the finite elements analysis.

1. Introduction

Shear deformation theory is a popular model in structural analysis. The displacement field is assumed as a polynomial of the thickness variable (z), which results in a system of differential equations without parameter z. By increasing the number of terms in the polynomial functions, it is possible to improve the approximate solution. Obviously, this leads to systems of differential equations which are more complex. The general form for displacement components in shear deformation theory is $U(x, y, z) = \sum_{i=0}^{n} u_i(x, y)z^i$ where $U(x, y, z)$ is the displacement component and $u_i(x, y)$ are unknown functions of the coordinates. For $i = 1$, one obtains first-order shear deformation theory (FSDT); $i = 2$ corresponds to second-order shear deformation theory (SSDT), and $i = 3$ gives third-order shear deformation theory (TSDT).

Although higher-order shear deformation theories can be used in the analysis of conical shells as well, most reported studies in this field are based on the classical theory of shells or the three-dimensional theory of elasticity and the governing equations have been solved numerically. Sundarasivarao and Ganesan [1991] analyzed a conical shell subjected to uniform internal pressure and various boundary conditions to find an optimum thickness variation by the finite element (FE) method. Sivadas and Ganesan [1991] studied the effects of thickness variation on the natural frequencies of laminated conical shells using a semianalytical FE method and Love's first approximation thin shell theory.

Panferov [1992] used the method of successive approximations and a perturbation of the shape of the boundary to determine the stress state of thick-walled conical isotropic shells with constant thickness subjected to thermal loading. Thambiratnam and Zhuge [1993] presented a simple FE method for the axisymmetric free vibration analysis of conical shells with uniform or varying wall thickness. Tong [1994] extracted equilibrium equations for the free vibration of composite laminated conical shells including transverse shear deformation and extension-bending coupling using a particularly convenient coordinate system. The solutions for the governing equations are in the form of a power series. Tavares [1996]

Keywords: shear deformation, stress analysis, finite elements, perturbation, thick shell, varying thickness.

determined the stresses, strains, and displacements of a thin conical shell with constant thickness and axisymmetric load by the construction of a Green's function for the homogeneous differential equation based on bending theory. Buchanan and Wong [2001] employed FE analysis to study the vibration of truncated thick hollow cones, using three-dimensional strain-displacement equations in a conical coordinate system.

Cui et al. [2001] introduced a new variable transformation to solve the basic governing differential equations for conical shells. By neglecting quantities with order of magnitude of h/R, the authors transformed the basic governing differential equations for conical shells into a second-order differential equation with complex coefficients. This equation has an accurate solution which is simpler than the exact solution because it does not use Bessel functions. Wu and Chiu [2002] investigated thermally induced dynamic instability of laminated composite conical shells subjected to static and periodic thermal loads by means of the multiple scales method of perturbation theory. Correia et al. [2003] presented a numerical method for the structural analysis of laminated conical shell panels using a quadrilateral isoparametric FE based on higher-order shear deformation theory. The displacement expressions used for the longitudinal and circumferential components of the displacement field were given by power series and a condition of zero stress on the top and bottom surfaces of the shell was imposed.

Garg et al. [2006] presented a FE model based on a TSDT for free vibration analysis of laminates. He concluded that applying the shear correction factor is not necessary. Ramesh et al. [2008] derived a triangular plate element based on higher-order shear deformation theory with superior performance through bending analysis of plates and examining the distribution of the stress resultants.

In this paper, displacements and stresses of a thick conical shell with varying thickness subjected to nonuniform internal pressure have been calculated using a TSDT for the homogeneous, isotropic, and axisymmetric cases. The governing equations, which are a system of differential equations with variable coefficients, have been solved analytically using the matched asymptotic expansion (MAE) of perturbation theory. The effects of different shear deformation theories on the displacements, von Mises stress, and shear stress have been studied. The results have been compared with FE analysis.

2. Governing equations

The coordinates of a point on the longitudinal section of a conical shell can be defined by the two parameters r and x, where x is the vertical coordinate, and r is the radius, which is perpendicular to x and satisfies $r = R(x) + z$. $R(x)$ is the middle surface radius, and z is the thickness variable, which is measured from the middle surface (see Figure 1). The displacement field in the axisymmetric case, based on TSDT, is assumed as

$$\begin{aligned} U_x(x,z) &= U_{x3} = u_0(x) + zu_1(x) + z^2u_2(x) + z^3u_3(x), \\ U_z(x,z) &= U_{z3} = w_0(x) + zw_1(x) + z^2w_2(x) + z^3w_3(x). \end{aligned} \tag{1}$$

U_x and U_z are the approximate axial and radial displacements, respectively, and u_0, u_1, u_2, u_3, w_0, w_1, w_2, and w_3 are the unknown functions of x. According to (1), the displacements vary cubically with respect to z and a cross section remains neither straight nor normal to the middle surface. The small-strain components are

$$
\begin{aligned}
e_x &= \frac{dU_x}{dx} = \frac{du_0}{dx} + z\frac{du_1}{dx} + z^2\frac{du_2}{dx} + z^3\frac{du_3}{dx},\\
e_z &= \frac{dU_z}{dz} = w_1 + 2zw_2 + 3z^2w_3,\\
e_\theta &= \frac{U_z}{r} = \frac{w_0 + zw_1 + z^2w_2 + z^3w_3}{R+z},\\
\gamma_{xz} &= \frac{dU_x}{dz} + \frac{dU_z}{dx} = u_1 + \frac{dw_0}{dx} + z\left(2u_2 + \frac{dw_1}{dx}\right) + z^2\left(3u_3 + \frac{dw_2}{dx}\right) + z^3\frac{dw_3}{dx}.
\end{aligned}
\tag{2}
$$

For an isotropic, homogeneous, linear elastic material, the stress-strain relations are

$$
\begin{aligned}
\sigma_x &= Ae_x + \lambda(e_\theta + e_z), \qquad & \sigma_z &= Ae_z + \lambda(e_\theta + e_x),\\
\sigma_\theta &= Ae_\theta + \lambda(e_x + e_z), \qquad & \sigma_{xz} &= \mu\gamma_{xz}.
\end{aligned}
\tag{3}
$$

Here λ and μ are the Lamé's constants and $A = \lambda + 2\mu$. The governing equations can be derived using the principal of virtual work which states that $\delta U = \delta W$. U is the strain energy and W is the external work. The variation of the strain energy for an axisymmetric elastic body is

$$
\delta U = \int_V (\sigma_{xx}\delta e_x + \sigma_{\theta\theta}\delta e_{\theta\theta} + \sigma_{zz}\delta e_{zz} + \sigma_{xz}\delta\gamma_{xz})\,dV, \tag{4}
$$

where V is the shell volume, $dV = r\,d\theta\,dx\,dz$, $0 \le \theta \le 2\pi$, $-h/2 \le z \le h/2$, and $0 \le x \le L$, with L the shell length and h the thickness. The external work variation due to internal pressure is

$$
\delta W = \iint_s (f_x\delta U_x + f_z\delta U_z)\,ds. \tag{5}
$$

ds is a surface element and f_x and f_z are the vertical and horizontal components of the pressure. After substituting (1)–(5) into the principal of virtual work and considering the coefficients of δu_0, δu_1, δu_2,

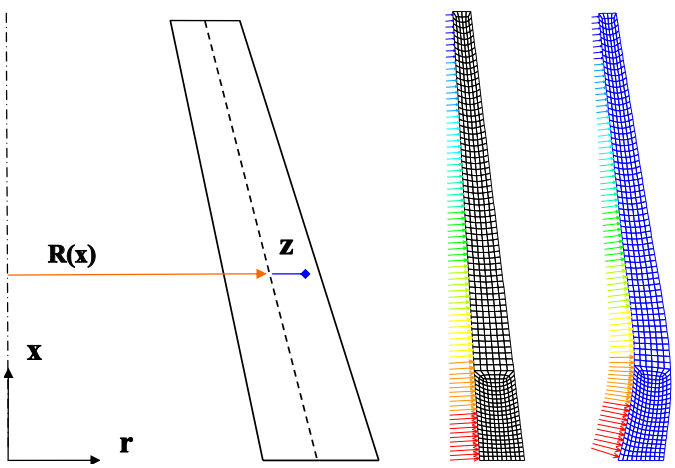

Figure 1. Shell geometry (left), loading (center), and deformation (right).

δu_3, δw_0, δw_1, δw_2, and δw_3, the results are

$$\begin{aligned}
\frac{d}{dx}(RN_x)+RF_{x_0}=0, \qquad & \frac{d}{dx}(RQ_x)-N_\theta+RF_{z_0}=0,\\
\frac{d}{dx}(RM_x)-RQ_x+RF_{x_1}=0, \qquad & \frac{d}{dx}(RM_{xz})-(M_\theta+RN_z)+RF_{z_1}=0,\\
\frac{d}{dx}(RP_x)-2RM_{xz}+RF_{x_2}=0, \qquad & \frac{d}{dx}(RP_{xz})-(P_\theta+2RM_z)+RF_{z_2}=0,\\
\frac{d}{dx}(RS_x)-3RP_{xz}+RF_{x_3}=0, \qquad & \frac{d}{dx}(RS_{xz})-(S_\theta+3RP_z)+RF_{z_3}=0,
\end{aligned} \tag{6}$$

where $F_{x_n}=f_x z^n\left(1+\frac{z}{R}\right)\Big|_{z=\pm\frac{h}{2}}$ and $F_{z_n}=f_z z^n\left(1+\frac{z}{R}\right)\Big|_{z=\pm\frac{h}{2}}$ for $n=0,1,2,3$, and the boundary conditions are

$$\left[R(N_x\delta u_0+M_x\delta u_1+P_x\delta u_2+S_x\delta u_3+Q_x\delta w_0+M_{xz}\delta w_1+P_{xz}\delta w_2+S_{xz}\delta w_3)\right]_{x=0}^{L}=0. \tag{7}$$

The first equation in (6) can be rewritten as $RN_x+\int RF_{x_0}dx+C_0=0$, and likewise the others.

The stress resultants are

$$\begin{aligned}
N_x&=\int_{-h/2}^{h/2}\sigma_x\left(1+\frac{z}{R}\right)dz\\
&=Ah\frac{du_0}{dx}+\frac{Ah^3}{12R}\frac{du_1}{dx}+\frac{Ah^3}{12}\frac{du_2}{dx}+\frac{Ah^5}{80R}\frac{du_3}{dx}+\frac{\lambda h}{R}w_0+\lambda h w_1+\frac{3\lambda h^3}{12R}w_2+\frac{3\lambda h^3}{12}w_3,\\
M_x&=\int_{-h/2}^{h/2}\sigma_x z\left(1+\frac{z}{R}\right)dz\\
&=\frac{Ah^3}{12R}\frac{du_0}{dx}+\frac{Ah^3}{12}\frac{du_1}{dx}+\frac{Ah^5}{80R}\frac{du_2}{dx}+\frac{Ah^5}{80}\frac{du_3}{dx}+\frac{2\lambda h^3}{12R}w_1+\frac{2\lambda h^3}{12}w_2+\frac{4\lambda h^5}{80R}w_3,\\
P_x&=\int_{-h/2}^{h/2}\sigma_x z^2\left(1+\frac{z}{R}\right)dz\\
&=\frac{Ah^3}{12}\frac{du_0}{dx}+\frac{Ah^5}{80R}\frac{du_1}{dx}+\frac{Ah^5}{80}\frac{du_2}{dx}+\frac{Ah^7}{448R}\frac{du_3}{dx}+\frac{\lambda h^3}{12R}w_0+\frac{\lambda h^3}{12}w_1+\frac{3\lambda h^5}{80R}w_2+\frac{3\lambda h^5}{80}w_3,\\
S_x&=\int_{-h/2}^{h/2}\sigma_x z^3\left(1+\frac{z}{R}\right)dz\\
&=\frac{Ah^5}{80R}\frac{du_0}{dx}+\frac{Ah^5}{80}\frac{du_1}{dx}+\frac{Ah^7}{448R}\frac{du_2}{dx}+\frac{Ah^7}{448}\frac{du_3}{dx}+\frac{2\lambda h^5}{80R}w_1+\frac{2\lambda h^5}{80}w_2+\frac{4\lambda h^7}{448R}w_3,\\
N_\theta&=\int_{-h/2}^{h/2}\sigma_\theta dz=A\alpha_0w_0+A\alpha_1w_1+\lambda h w_1+A\alpha_2w_2+A\alpha_3w_3+\frac{3\lambda h^3}{12}w_3+\lambda h\frac{du_0}{dx}+\frac{\lambda h^3}{12}\frac{du_2}{dx},\\
M_\theta&=\int_{-h/2}^{h/2}\sigma_\theta z dz=A\alpha_1w_0+A\alpha_2w_1+A\alpha_3w_2+A\alpha_4w_3+\frac{2\lambda h^3}{12}w_2+\frac{\lambda h^3}{12}\frac{du_1}{dx}+\frac{\lambda h^5}{80}\frac{du_3}{dx},\\
P_\theta&=\int_{-h/2}^{h/2}\sigma_\theta z^2 dz=A\alpha_2w_0+A\alpha_3w_1+A\alpha_4w_2+A\alpha_5w_3+\frac{\lambda h^3}{12}w_1+\frac{3\lambda h^5}{80}w_3+\frac{\lambda h^3}{12}\frac{du_0}{dx}+\frac{\lambda h^5}{80}\frac{du_2}{dx},\\
S_\theta&=\int_{-h/2}^{h/2}\sigma_\theta z^3 dz=A\alpha_3w_0+A\alpha_4w_1+A\alpha_5w_2+A\alpha_6w_3+\frac{2\lambda h^5}{80}w_2+\frac{\lambda h^5}{80}\frac{du_1}{dx}+\frac{\lambda h^7}{488}\frac{du_3}{dx},
\end{aligned}$$

$$
\begin{aligned}
N_z &= \int_{-h/2}^{h/2} \sigma_z \Big(1+\frac{z}{R}\Big)\,dz \\
&= \frac{\lambda h}{R} w_0 + A h w_1 + \frac{(2A+\lambda)h^3}{12R} w_2 + \frac{3Ah^3}{12} w_3 + \lambda h \frac{du_0}{dx} + \frac{\lambda h^3}{12R}\frac{du_1}{dx} + \frac{\lambda h^3}{12}\frac{du_2}{dx}, \\
M_z &= \int_{-h/2}^{h/2} \sigma_z z \Big(1+\frac{z}{R}\Big)\,dz \\
&= \frac{(A+\lambda)h^3}{12R} w_1 + \frac{2Ah^3}{12} w_2 + \frac{(3A+\lambda)h^5}{80R} w_3 + \frac{\lambda h^3}{12R}\frac{du_0}{dx} + \frac{\lambda h^3}{12}\frac{du_1}{dx} + \frac{\lambda h^5}{80R}\frac{du_2}{dx} + \frac{\lambda h^5}{80}\frac{du_3}{dx}, \\
P_z &= \int_{-h/2}^{h/2} \sigma_z z^2 \Big(1+\frac{z}{R}\Big)\,dz \\
&= \frac{\lambda h^3}{12R} w_0 + \frac{Ah^3}{12} w_1 + \frac{(2A+\lambda)h^5}{80R} w_2 + \frac{3Ah^5}{80} w_3 + \frac{\lambda h^3}{12}\frac{du_0}{dx} + \frac{\lambda h^5}{80R}\frac{du_1}{dx} + \frac{\lambda h^5}{80}\frac{du_2}{dx} + \frac{\lambda h^7}{448R}\frac{du_3}{dx}, \\
Q_x &= \int_{-h/2}^{h/2} \sigma_{xz} \Big(1+\frac{z}{R}\Big)\,dz \\
&= \mu\Big\{ h u_1 + \frac{2h^3}{12R} u_2 + \frac{3h^3}{12} u_3 + h\frac{dw_0}{dx} + \frac{h^3}{12R}\frac{dw_1}{dx} + \frac{h^3}{12}\frac{dw_2}{dx} + \frac{h^5}{80R}\frac{dw_3}{dx}\Big\}, \\
M_{xz} &= \int_{-h/2}^{h/2} \sigma_{xz} z \Big(1+\frac{z}{R}\Big)\,dz \\
&= \mu\Big\{ \frac{h^3}{12R} u_1 + \frac{2h^3}{12} u_2 + \frac{3h^5}{80R} u_3 + \frac{h^3}{12R}\frac{dw_0}{dx} + \frac{h^3}{12}\frac{dw_1}{dx} + \frac{h^5}{80R}\frac{dw_2}{dx} + \frac{h^5}{80}\frac{dw_3}{dx}\Big\}, \\
P_{xz} &= \int_{-h/2}^{h/2} \sigma_{xz} z^2 \Big(1+\frac{z}{R}\Big)\,dz \\
&= \mu\Big\{ \frac{h^3}{12} u_1 + \frac{2h^5}{80R} u_2 + \frac{3h^5}{80} u_3 + \frac{h^3}{12}\frac{dw_0}{dx} + \frac{h^5}{80R}\frac{dw_1}{dx} + \frac{h^5}{80}\frac{dw_2}{dx} + \frac{h^7}{448R}\frac{dw_3}{dx}\Big\}, \\
S_{xz} &= \int_{-h/2}^{h/2} \sigma_{xz} z^3 \Big(1+\frac{z}{R}\Big)\,dz \\
&= \mu\Big\{ \frac{h^5}{80R} u_1 + \frac{2h^5}{80} u_2 + \frac{3h^7}{448R} u_3 + \frac{h^5}{80R}\frac{dw_0}{dx} + \frac{h^5}{80}\frac{dw_1}{dx} + \frac{h^7}{448R}\frac{dw_2}{dx} + \frac{h^7}{448}\frac{dw_3}{dx}\Big\}. \qquad (8)
\end{aligned}
$$

By assuming $v = du_0/dx$ and using (6) and (8), we derive the governing equations in terms of the displacement parameters:

$$
\frac{d}{dx}\Big([A_1]\frac{d\{Y\}}{dx}\Big) + \frac{d}{dx}\big([A_2]\{Y\}\big) + [A_3]\frac{d\{Y\}}{dx} + [A_4]\{Y\} + \{F_p\} = \{0\}_{8\times 1}, \qquad (9a)
$$

where

$$
\{F_p\} = \{RF_{x_0} + C_0, RF_{x_1}, RF_{x_2}, RF_{x_3}, RF_{z_0}, RF_{z_1}, RF_{z_2}, RF_{z_3}\}^T,
$$

$$
A_1 = \begin{bmatrix} [A_{11}]_{4*4} & [0]_{4*4} \\ [0]_{4*4} & \theta_2[A_{14}]_{4*4} \end{bmatrix}, \qquad A_2 = \begin{bmatrix} [0]_{4*4} & \theta_1[A_{22}]_{4*4} \\ \theta_2[A_{23}]_{4*4} & [0]_{4*4} \end{bmatrix},
$$

$$
A_3 = \begin{bmatrix} [A_{31}]_{4*4} & -\theta_2[A_{32}]_{4*4} \\ -\theta_1[A_{33}]_{4*4} & [0]_{4*4} \end{bmatrix}, \qquad A_4 = \begin{bmatrix} -\theta_2[A_{41}]_{4*4} & \theta_1[A_{42}]_{4*4} \\ -\theta_1[A_{42}]^T_{4*4} & -[A_{44}]_{4*4} \end{bmatrix},
$$

$$[A_{11}]_{4*4}=\begin{bmatrix}0&0&0&0\\0&\frac{Rh^3}{12}&\frac{h^5}{80}&\frac{Rh^5}{80}\\0&\frac{h^5}{80}&\frac{Rh^5}{80}&\frac{h^7}{448}\\0&\frac{Rh^5}{80}&\frac{h^7}{448}&\frac{Rh^7}{448}\end{bmatrix},\qquad [A_{14}]_{4*4}=\begin{bmatrix}Rh&\frac{h^3}{12}&\frac{Rh^3}{12}&\frac{h^5}{80}\\\frac{h^3}{12}&\frac{Rh^3}{12}&\frac{h^5}{80}&\frac{Rh^5}{80}\\\frac{Rh^3}{12}&\frac{h^5}{80}&\frac{Rh^5}{80}&\frac{h^7}{448}\\\frac{h^5}{80}&\frac{Rh^5}{80}&\frac{h^7}{448}&\frac{Rh^7}{448}\end{bmatrix},$$

$$[A_{22}]_{4*4}=\begin{bmatrix}0&0&0&0\\0&\frac{2h^3}{12}&\frac{2Rh^3}{12}&\frac{4h^5}{80}\\\frac{h^3}{12}&\frac{Rh^3}{12}&\frac{3h^5}{80}&\frac{3Rh^5}{80}\\0&\frac{2h^5}{80}&\frac{2Rh^5}{80}&\frac{4h^7}{448}\end{bmatrix},\qquad [A_{23}]_{4*4}=\begin{bmatrix}0&Rh&\frac{2h^3}{12}&\frac{3Rh^3}{12}\\0&\frac{h^3}{12}&\frac{2Rh^3}{12}&\frac{3h^5}{80}\\0&\frac{Rh^3}{12}&\frac{2h^5}{80}&\frac{3Rh^5}{80}\\0&\frac{h^5}{80}&\frac{2Rh^5}{80}&\frac{3h^7}{448}\end{bmatrix},$$

$$[A_{31}]_{4*4}=\begin{bmatrix}0&\frac{h^3}{12}&\frac{Rh^3}{12}&\frac{h^5}{80}\\0&0&0&0\\0&0&0&0\\0&0&0&0\end{bmatrix},\qquad [A_{32}]_{4*4}=\begin{bmatrix}0&0&0&0\\Rh&\frac{h^3}{12}&\frac{Rh^3}{12}&\frac{h^5}{80}\\\frac{2h^3}{12}&\frac{2Rh^3}{12}&\frac{2h^5}{80}&\frac{2Rh^5}{80}\\\frac{3Rh^3}{12}&\frac{3h^5}{80}&\frac{3Rh^5}{80}&\frac{3h^7}{448}\end{bmatrix},$$

$$[A_{33}]_{4*4}=\begin{bmatrix}0&0&\frac{h^3}{12}&0\\0&\frac{2h^3}{12}&\frac{Rh^3}{12}&\frac{2h^5}{80}\\0&\frac{2Rh^3}{12}&\frac{3h^5}{80}&\frac{2Rh^5}{80}\\0&\frac{4h^5}{80}&\frac{3Rh^5}{80}&\frac{4h^7}{448}\end{bmatrix},\qquad [A_{41}]_{4*4}=\begin{bmatrix}\frac{-Rh}{\theta_2}&0&0&0\\0&Rh&\frac{2h^3}{12}&\frac{3Rh^3}{12}\\0&\frac{2h^3}{12}&\frac{4Rh^3}{12}&\frac{6h^5}{80}\\0&\frac{3Rh^3}{12}&\frac{6h^5}{80}&\frac{9Rh^5}{80}\end{bmatrix},$$

$$[A_{42}]_{4*4}=\begin{bmatrix}h&Rh&\frac{h^3}{4}&\frac{Rh^3}{4}\\0&0&0&0\\0&0&0&0\\0&0&0&0\end{bmatrix},\quad \theta_1=\frac{\lambda}{A},\quad \theta_2=\frac{\mu}{A},\quad \alpha_n=\int_{-h/2}^{h/2}\frac{z^n dz}{R+z},\quad n=0,\dots,6,$$

$$[A_{44}]_{4*4}=\begin{bmatrix}\alpha_0&\alpha_1+\theta_1 h&\alpha_2&\alpha_3+\theta_1\frac{3h^3}{12}\\\alpha_1+\theta_1 h&\alpha_2+Rh&\alpha_3+(3\theta_1+2)\frac{h^3}{12}&\alpha_4+\frac{3Rh^3}{12}\\\alpha_2&\alpha_3+(3\theta_1+2)\frac{h^3}{12}&\alpha_4+\frac{4Rh^3}{12}&\alpha_5+(5\theta_1+6)\frac{h^5}{80}\\\alpha_3+\theta_1\frac{3h^3}{12}&\alpha_4+\frac{3Rh^3}{12}&\alpha_5+(5\theta_1+6)\frac{h^5}{80}&\alpha_6+\frac{9Rh^5}{80}\end{bmatrix}. \tag{9b}$$

Equations (9a) and (9b) were derived by assuming (1) as the displacement field, but it is possible to consider different theories of shear deformation, and in each case only the coefficient matrices A_i change. In this paper the results of nine cases have been studied. By the definition of the functions, we have

$$\begin{aligned} U_{x2} &= u_0(x) + zu_1(x) + z^2u_2(x), & U_{x1} &= u_0(x) + zu_1(x), \\ U_{z2} &= w_0(x) + zw_1(x) + z^2w_2(x), & U_{z1} &= w_0(x) + zw_1(x). \end{aligned} \tag{10}$$

These are the nine cases studied:

$$\begin{aligned} &\text{Case 1:} && U_x(x,z) = Ux_3, && Uz(x,z) = Uz_3 && \rightarrow && \text{VMS}_{33}, Sxz_{33}, \\ &\text{Case 2:} && U_x(x,z) = Ux_3, && Uz(x,z) = Uz_2 && \rightarrow && \text{VMS}_{32}, Sxz_{32}, \\ &\text{Case 3:} && U_x(x,z) = Ux_3, && Uz(x,z) = Uz_1 && \rightarrow && \text{VMS}_{31}, Sxz_{31}, \\ &\text{Case 4:} && U_x(x,z) = Ux_2, && Uz(x,z) = Uz_3 && \rightarrow && \text{VMS}_{23}, Sxz_{23}, \\ &\text{Case 5:} && U_x(x,z) = Ux_2, && Uz(x,z) = Uz_2 && \rightarrow && \text{VMS}_{22}, Sxz_{22}, \\ &\text{Case 6:} && U_x(x,z) = Ux_2, && Uz(x,z) = Uz_1 && \rightarrow && \text{VMS}_{21}, Sxz_{21}, \\ &\text{Case 7:} && U_x(x,z) = Ux_1, && Uz(x,z) = Uz_3 && \rightarrow && \text{VMS}_{13}, Sxz_{13}, \\ &\text{Case 8:} && U_x(x,z) = Ux_1, && Uz(x,z) = Uz_2 && \rightarrow && \text{VMS}_{12}, Sxz_{12}, \\ &\text{Case 9:} && U_x(x,z) = Ux_1, && Uz(x,z) = Uz_1 && \rightarrow && \text{VMS}_{11}, Sxz_{11}, \end{aligned} \tag{11}$$

where VMS stands for the von Mises stress and Sxz is the shear stress due to the selected displacement field. The governing equations for all nine cases are (9a) but the coefficient matrices A_i will change by the removal of some entries. For example, by applying $w_3 = 0$ to (9a), the equilibrium equations for case 2 are obtained. This corresponds to omitting the eighth column and row of the coefficient matrices and neglecting the eighth element of the force and displacement vectors, or, for case 7, removing the third and fourth rows and columns of the matrices and the third and fourth elements of the displacement and force vectors. This is in agreement with the results obtained in [Eipakchi et al. 2008].

Equation (9a) is a system of ordinary differential equations with variable coefficients. Frobenius series are the usual method for solving this kind of equations. This method has slow convergence and needs a lot of calculations. Also, one must know the inner and outer profiles of the shell and loading distribution, *before formulation*.

3. Analytical solution

In this paper, the MAE method has been used for solving the governing equations, which are a system of differential equations with variable coefficients. This method does not require knowledge of the inner and outer profiles of the shell and loading distribution before formulation, and can explain the behavior of the shell successfully even near the boundaries. The convergence of the solution is quick. The method involves solving a system of algebraic equations and two systems of differential equations with constant coefficients. These systems of equations have closed-form solutions.

We start by making the governing equations dimensionless, using the following characteristic scales:

$$x^* = \frac{x}{L}, \quad R^* = \frac{R}{h_0}, \quad h^* = \frac{h}{h_0}, \quad u_2^* = u_2h_0, \quad u_3^* = u_3h_0^2, \quad w_0^* = \frac{w_0}{h_0}, \quad w_2^* = w_2h_0, \quad w_3^* = w_3h_0^2, \tag{12}$$

where h_0 is the thickness characteristic and u_2^*, u_3^*, w_2^*, and w_3^* are the unknown dimensionless functions of x^*. By using these functions, the displacement field (1) converts to a nondimensional form as $U_z^* = U_z/h_0$ and $U_x^* = U_x/h_0$. By substituting (12) into (9), the nondimensional form of (9) is obtained:

$$\varepsilon^2 \frac{d}{dx^*}\left([A_1^*]\frac{d\{Y^*\}}{dx^*}\right) + \varepsilon\left(\frac{d}{dx^*}\left([A_2^*]\{Y^*\}\right) + [A_3^*]\frac{d\{Y^*\}}{dx^*}\right) + [A_4^*]\{Y^*\} + \frac{1}{\varepsilon}\{F_1^*\} + \{F_2^*\} = \{0\}. \quad (13a)$$

Here $\varepsilon = h_0/L$ is assumed small and will be taken as the perturbation parameter; The matrices $[A_i^*]$, $i = 1, \ldots, 4$, which are functions of x^*, are determined by replacing R with R^* and h with h^* in the matrices $[A_i]$, $i = 1, \ldots, 4$. The vectors $\{Y^*\}$, $\{F_1^*\}$, and $\{F_2^*\}$ are

$$\begin{aligned} &\{Y^*\} = \{v, u_1, u_2^*, u_3^*, w_0^*, w_1, w_2^*, w_3^*\}^T, \qquad \{F_1^*\} = \left\{\int \frac{R^*}{A} F_{x_0}\, dx^*, 0, 0, 0, 0, 0, 0, 0\right\}^T, \\ &\{F_2^*\} = \{C_0^*, F_{x_1}^*, F_{x_2}^*, F_{x_3}^*, F_{z_0}^*, F_{z_1}^*, F_{z_2}^*, F_{z_3}^*\}^T, \qquad F_k^* = \frac{R^* F_k}{A}, \quad k = x_1, x_2, x_3, z_0, z_1, z_2, z_3, \end{aligned} \quad (13b)$$

where C_0^* is a constant.

Equation (13a) suggest that there are two boundary layers, one at each end of the shell. So, the solution of the problem contains an outer expansion away from the boundaries and two inner expansions near the two boundaries [Nayfeh 1981, Chapter 12].

3.1. ***Outer expansion.*** This solution is considered as a uniform series of ε:

$$\{Y_{\text{out}}^*\} = \frac{1}{\varepsilon^\nu}\left(\{y_0(x^*)\} + \varepsilon\{y_1(x^*)\} + \varepsilon^2\{y_2(x^*)\} + \cdots\right). \quad (14)$$

Substituting (14) into (13) and considering the dominant terms, one obtains $\nu = 1$ (distinguished limit), so the equations with the same orders are

$$\begin{aligned} O(\varepsilon^{-1}): &\quad [A_4^*]\{y_0\} + \{F_1^*\} = \{0\}_{8*1}, \\ O(\varepsilon^{0}): &\quad [A_4^*]\{y_1\} + \frac{d}{dx^*}\left([A_2^*]\{y_0\}\right) + [A_3^*]\frac{d\{y_0\}}{dx^*} + \{F_2^*\} = \{0\}_{8*1}, \\ O(\varepsilon^{1}): &\quad [A_4^*]\{y_2\} + \frac{d}{dx^*}\left([A_2^*]\{y_1\}\right) + [A_3^*]\frac{d\{y_1\}}{dx^*} + \frac{d}{dx^*}\left([A_1^*]\frac{d\{y_0\}}{dx^*}\right) = \{0\}_{8*1}. \end{aligned} \quad (15)$$

Equations (15) are systems of algebraic equations, which are responsible for the shell away from the boundaries.

3.2. ***Inner expansion at x* = 0.*** The fast variable $\eta = x^*/\varepsilon$ is taken as the new variable for this region. The Taylor expansions of the coefficient matrices around $\varepsilon = 0$ are as follows:

$$\begin{aligned} &[A_i^*(x^*)] = [A_i^*(0)] + \varepsilon\eta[a_i] + \varepsilon^2\eta^2[d_i] + \cdots, && i = 1, \ldots, 4, \\ &\{F_j^*(x^*)\} = \{F_j^*(0)\} + \varepsilon\eta\left.\frac{d\{F_j^*\}}{dx^*}\right|_{x^*=0} + \frac{1}{2}\varepsilon^2\eta^2\left.\frac{d^2\{F_j^*\}}{dx^{*2}}\right|_{x^*=0} + \cdots, && j = 1, 2, \end{aligned} \quad (16)$$

where

$$[a_k] = \left.\frac{d[A_k^*]}{dx^*}\right|_{x^*=0}, \qquad [d_k] = \frac{1}{2}\left.\frac{d^2[A_k^*]}{dx^{*2}}\right|_{x^*=0}, \qquad k = 1, \ldots, 4.$$

The solution in this region is sought in the form

$$\{Y^*_{\text{in}}\} = \frac{1}{\varepsilon}\big(\{y_0(\eta)\} + \varepsilon\{y_1(\eta)\} + \varepsilon^2\{y_2(\eta)\} + \cdots\big), \tag{17}$$

and by substituting (16) and (17) into (13a), the terms of same order are collected as

$$O(\varepsilon^{-1}) : \big\{L_1(\{y_0\},\eta,0)\big\} + \{F_1^*(0)\} = \{0\}_{8*1}, \tag{18a}$$

$$O(\varepsilon^{0}) : \big\{L_1(\{y_1\},\eta,0)\big\} + \big\{M_1(\{y_0\},\eta,[a_1],[a_2],[a_3],[a_4],0)\big\} + \eta\frac{d\{F_1^*\}}{dx^*}\bigg|_{x^*=0} + \{F_2^*(0)\} = \{0\}_{8*1}, \tag{18b}$$

$$O(\varepsilon^{1}) : \big\{L_1(\{y_2\},\eta,0)\big\} + \big\{M_1(\{y_1\},\eta,[a_1],[a_2],[a_3],[a_4],0)\big\} + \big\{M_1(\{y_0\},\eta,[d_1],[d_2],[d_3],[d_4],0)\big\} + \eta\frac{d\{F_2^*\}}{dx^*}\bigg|_{x^*=0} + \frac{1}{2}\eta^2\frac{d^2\{F_1^*\}}{dx^{*2}}\bigg|_{x^*=0} = \{0\}_{8*1}, \tag{18c}$$

where the differential operators $\{L_1\}$ and $\{M_1\}$ are given by

$$\begin{aligned}\big\{M_1(\{y\},x,[a_1],[a_2],[a_3],[a_4],j)\big\} &= [a_1]\frac{d}{dx}\Big(x\frac{d\{y\}}{dx}\Big) + [a_2]\frac{d}{dx}\big(x\{y\}\big) + [a_3]x\frac{d\{y\}}{dx} + [a_4]x\{y\},\\ \big\{L_1(\{y\},x,i)\big\} &= [A_1^*(i)]\frac{d^2\{y\}}{dx^2} + \big([A_2^*(i)] + [A_3^*(i)]\big)\frac{d\{y\}}{dx} + [A_4^*(i)]\{y\};\end{aligned} \tag{19}$$

Equations (18), which are systems of ordinary differential equations with constant coefficients, are solved using the elementary theory of differential equations [Wylie 1979].

3.3. ***Inner expansion at $x^* = 1$.*** The fast variable $\xi = (x^*-1)/\varepsilon$ is taken as the new variable for this region. The Taylor expansions of the coefficient matrices around $\varepsilon = 0$ are

$$\begin{aligned}[A_i^*(x^*)] &= [A_i^*(1)] + \varepsilon\xi[a_i] + \varepsilon^2\xi^2[d_i] + \cdots, && i = 1,\ldots,4,\\ \{F_j^*(x^*)\} &= \{F_j^*(1)\} + \varepsilon\xi\frac{d\{F_j^*\}}{dx^*}\bigg|_{x^*=1} + \frac{1}{2}\varepsilon^2\xi^2\frac{d^2\{F_j^*\}}{dx^{*2}}\bigg|_{x^*=1} + \cdots, && j = 1,2,\end{aligned} \tag{20}$$

where

$$[a_k] = \frac{d[A_k^*]}{dx^*}\bigg|_{x^*=1}, \qquad [d_k] = \frac{1}{2}\frac{d^2[A_k^*]}{dx^{*2}}\bigg|_{x^*=1}, \qquad k = 1,\ldots,4.$$

We consider the solution

$$\{Y^*_{IN}\} = \frac{1}{\varepsilon}\big(\{y_0(\xi)\} + \varepsilon\{y_1(\xi)\} + \varepsilon^2\{y_2(\xi)\} + \cdots\big). \tag{21}$$

By substituting (20) and (21) into (13a), the same-order terms are

$$O(\varepsilon^{-1}) : \big\{L_1(\{y_0\},\xi,1)\big\} + \{F_1^*(1)\} = \{0\}_{8*1}, \tag{22a}$$

$$O(\varepsilon^{0}) : \big\{L_1(\{y_1\},\xi,1)\big\} + \big\{M_1(\{y_0\},\xi,[a_1],[a_2],[a_3],[a_4],1)\big\} + \xi\frac{d\{F_1^*\}}{dx^*}\bigg|_{x^*=1} + \{F_2^*(1)\} = \{0\}_{8*1}, \tag{22b}$$

$$O(\varepsilon^1): \big\{L_1\big(\{y_2\},\xi,1\big)\big\}+\big\{M_1\big(\{y_1\},\xi,[a_1],[a_2],[a_3],[a_4],1\big)\big\}$$
$$+\big\{M_1\big(\{y_0\},\xi,[d_1],[d_2],[d_3],[d_4],1\big)\big\}+\xi\frac{d\{F_2^*\}}{dx^*}\bigg|_{x^*=1}+\tfrac{1}{2}\xi^2\frac{d^2\{F_1^*\}}{dx^{*2}}\bigg|_{x^*=1}=\{0\}_{8*1}. \quad (22c)$$

Equations (22) forms a set of coupled ordinary differential equations with constant coefficients, and one can solve these equations as in the last section.

3.4. ***Composite solution.*** In the MAE method, the composite solution is the summation of these three calculated solutions minus the overlapping parts of them:

$$\{Y^*\}=\{Y^*_{\text{in}}\}+\{Y^*_{\text{IN}}\}+\{Y^*_{\text{out}}\}-\big(\{J_0\}+\{J_L\}\big). \quad (23)$$

$\{J_0\}$ and $\{J_L\}$ are the common parts of the inner and outer solutions at the two ends of the shell and can be determined by van Dyke's matching principle [Nayfeh 1981, pp. 282–283].

4. Case studies

A thick cylinder with constant thickness subjected to constant internal pressure. By solving this problem, it is possible to find a validation range of thickness to use the shear deformation theory in the stress and displacement analysis of a thick cylinder. Away from the boundaries, the solution can be found with Lamé's formula, which is an exact solution. According to Lamé's formula, the radial and hoop stresses are $\sigma_r = c_1 + c_2/r^2$ and $\sigma_\theta = c_1 - c_2/r^2$. The constants c_1 and c_2 are determined from the boundary conditions: the inner wall is subjected to internal pressure and the outer wall is traction free. By using Hooke's law, the radial and axial displacements in the plane stress state are $U_z = c_3 r + c_4/r$ and $U_x = c_5 x$ where c_3, c_4, and c_5 are constants that depend on the geometrical and material properties of the cylinder. So, it is possible to estimate the von Mises stress easily. Away from the boundaries, the solution of this problem can be obtained with (15), which is the solution of the algebraic equations $[A_4]\{Y\}+\{F_p\}=\{0\}$. Thus the parameters in (1) are $u_1 = u_2 = u_3 = 0$, $u_0 = c_6 x$, and w_0, w_1, w_2, and w_3 are calculated. For this problem, the nine cases in (11) reduce to just the three following cases:

$$\begin{aligned}
&\text{Case 1:}\quad U_x(x,z)=c_6x,\quad U_z(x,z)=U_{z3}\quad\rightarrow\quad VMS_{33},\\
&\text{Case 2:}\quad U_x(x,z)=c_6x,\quad U_z(x,z)=U_{z2}\quad\rightarrow\quad VMS_{32},\\
&\text{Case 3:}\quad U_x(x,z)=c_6x,\quad U_z(x,z)=U_{z1}\quad\rightarrow\quad VMS_{31}.
\end{aligned} \quad (24)$$

The axial displacement depends on the selected radial displacement field or it depends on z, implicitly. By comparing these solutions, one can determine the relative difference between exact and approximate solutions, that is, the quotient $(q_{\text{exact}} - q_{\text{shear}})/q_{\text{exact}}$ (expressed as a percentage), where q is the quantity of interest at the *inner wall* of the shell, and the subscripts "exact" and "shear" stand for the Lamé and shear deformation solutions. Figure 2, top, plots the relative difference in radial displacement versus $m = R/h$ for the theories listed in (24). As the thickness decreases, so does the relative difference; for $m > 4$ there is nearly no advantage to higher-order theories. For thick shells, TSDT shows a smaller difference.

Figure 2, bottom, shows the difference percentage of the von Mises stress for values of m. FSDT is a poor approximation for the von Mises stress, and TSDT is very good for thick shells. For moderately thick shells (for instance, $m > 4$), there is no difference between SSDT and TSDT.

Figure 3 compares the quantity $E \cdot U_x/(p \cdot x)$ with respect to m with different theories where p is the internal pressure. Approximately, TSDT and SSDT are the same for the axial displacement prediction.

A thick conical shell with varying thickness subjected to nonuniform internal pressure. Table 1, on the next page, lists the geometrical and material properties of the shell. The variation of the pressure is linear and the boundary conditions are clamped-free (see Figure 1). The MAE method has been used for the stress analysis of this shell. The calculations were performed on Maple 10 software, and were based on TSDT. From this solution, it is possible to extract the nine cases of (11).

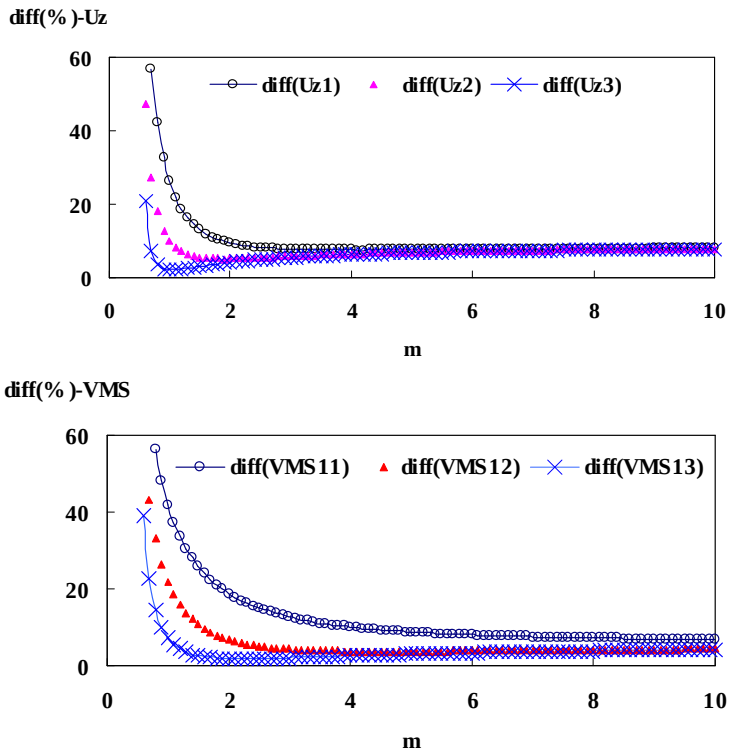

Figure 2. Relative difference in the radial displacement (top) and the von Mises stress (bottom) as a function of m. See (24) for the meaning of the three cases.

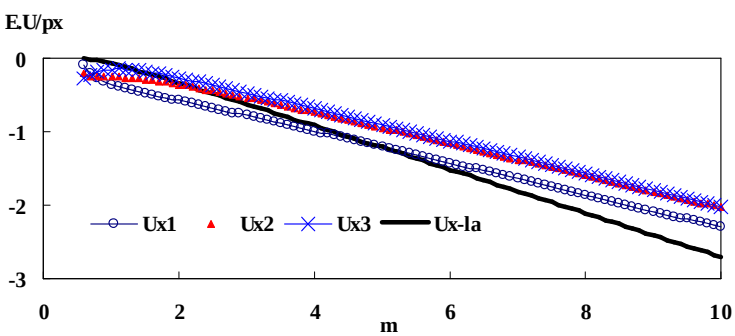

Figure 3. Nondimensional axial displacement as a function of m. See (24).

Shell length	$L = 50\,\text{cm}$
Inner radius at $x = 0$	$R_{i0} = 10\,\text{cm}$
Inner radius at $x = L$	$7\,\text{cm}$
Outer radius at $x = 0$	$15\,\text{cm}$
Outer radius at $x = L$	$9\,\text{cm}$
Internal pressure at $x = 0$	$P_0 = 200\,\text{MPa}$
Internal pressure at $x = L$	$50\,\text{MPa}$
Young's modulus	$E = 210\,\text{GPa}$
Poisson's ratio	0.3

Table 1. Shell properties.

Outer expansion. This is the solution of (15). Although the solution is straightforward, by increasing the order of ε, calculation time increases due to enlarging the nonhomogeneous part of equations. It is possible to decrease running time by special programming techniques.

Inner solution. At $x^* = 0$, this is the solution of (18). It is in the form of systems of nonhomogeneous ordinary differential equations with constant coefficients. The general solution is $\{y\} = \{V\}e^{\lambda_i \eta}$, where $\{V\}$ is the eigenvector and λ_i is the eigenvalue. By substituting the general solution in the homogeneous part of (18a), we find

$$\big(A_1^*(0)\lambda_i^2 + \big[A_2^*(0) + A_3^*(0)\big]\lambda_i + A_4^*(0)\big)\{V\} = \{0\}. \tag{25}$$

λ_i is calculated from the determinant of the system matrix, that is,

$$\det\big(A_1^*(0)\lambda_i^2 + \big[A_2^*(0) + A_3^*(0)\big]\lambda_i + A_4^*(0)\big) = 0.$$

This equation has 14 roots and for each root, an eigenvector can be calculated from (25). So the general solution is

$$\{y\}_g = \sum_{i=1}^{14} C_i\{V_i\}e^{\lambda_i \eta},$$

which is valid for (18). The particular solution of (18a) depends on the nonhomogeneous part, which is a constant vector and can be considered as $\{y\}_p = \{K_0\}$. By substituting this solution into (18a), $\{K_0\}$ is determined. The total solution is $\{y\} = \{y\}_g + \{y\}_p$. There are 14 constants. Seven constants, which correspond to eigenvalues with positive real parts, are zero, because the solution is finite at $\eta \to \infty$. The remaining constants are determined from the clamped boundary conditions at $x^* = 0$ for this case study, that is, $u_1 = u_2^* = u_3^* = w_0^* = w_1 = w_2^* = w_3^* = 0$. The condition $u_0 = 0$ is applied, later. The particular solution of (18b) is

$$\{y\}_p = \sum_{i=1}^{7} \big(\{K_{0i}\} + \{K_{1i}\}\eta + \{K_{2i}\}\eta^2\big)e^{\lambda_i \eta} + \{K_1\}\eta + \{K_0\},$$

and by substituting this solution into (18b), the unknown vectors can be determined. The boundary conditions are applied to the total solution of this order to determine seven constants. The particular

solution of (18c) is

$$\{y\}_p = \sum_{i=1}^{7}\left(\{K_{0i}\}+\{K_{1i}\}\eta+\{K_{2i}\}\eta^2+\{K_{3i}\}\eta^3+\{K_{4i}\}\eta^4\right)e^{\lambda_i\eta}+\{K_2\}\eta^2+\{K_1\}\eta+\{K_0\},$$

and by substituting into (18c), the coefficient vectors are determined. Seven constants are determined from the clamped boundary conditions.

Inner solution. At $x^* = 1$, this is the solution of (22), which are in the form of systems of nonhomogeneous ordinary differential equations with constant coefficients. The general solution for each system is

$$\{y\}_g = \sum_{i=1}^{14} C_i\{V_i\}e^{\lambda_i\xi}.$$

The eigenvalues λ_i are the roots of algebraic equation

$$\det\left(A_1^*(1)\lambda_i^2+\left[A_2^*(1)+A_3^*(1)\right]\lambda_i+A_4^*(1)\right)=0,$$

and the eigenvectors $\{V\}$ are determined from

$$\left(A_1^*(1)\lambda_i^2+\left[A_2^*(1)+A_3^*(1)\right]\lambda_i+A_4^*(1)\right)\{V\}=\{0\}.$$

The particular solution of (22a) is $\{y\}_p = \{K_0\}$ and the total solution is $\{y\} = \{y\}_g + \{y\}_p$. Seven constants, which correspond to eigenvalues with negative real parts, are zero because the solution is finite at $\xi \to -\infty$. The other constants are determined from the free boundary conditions at $x^* = 1$ for this case study, that is, $M_x = P_x = S_x = Q_x = M_{xz} = P_{xz} = S_{xz} = 0$. The condition $N_x = 0$ is applied later. The particular solutions of (22b) and (22c) are similar to the case of the previous section, except that the variable is ξ.

Composite solution. This solution is determined from (23) for each order of ε. The common parts were specified by removing the exponential terms of the inner solutions for this case study. By integrating the first element of (23), u_0 is calculated and a new constant of integration is found. This constant and C_0^* are calculated from the clamped-free boundary conditions. At $x = 0$, $u_0 = 0$, and at $x = L$, $N_x = 0$.

5. Numerical results

The ANSYS 5.4 FE package was used in the static analysis of this thick conical shell with varying thickness. The PLANE82 element in axisymmetric mode, which is an element with eight nodes and two translational degrees of freedom in the axial and radial directions per each node, was used for discretization. The boundary conditions were considered clamped-free and the characteristics of the shell have been listed in Table 1. Figure 1 shows the loading, mesh pattern, and deformation of the shell.

6. Comparison of results

Figure 4 shows the radial displacement of the inner wall for different orders of ε. It is seen that order (ε^{-1}) is not an acceptable solution, but orders $(\varepsilon^1, \varepsilon^0)$ have a good convergence. There is not any noticeable difference between these orders. This result is valid for the axial displacement and the von Mises stress. So, the displacements and the von Mises stress have been calculated with the order (ε^0) expansion for

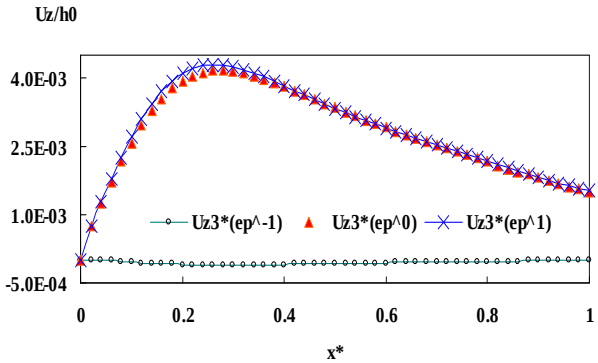

Figure 4. Convergence procedure for radial displacement by different expansions.

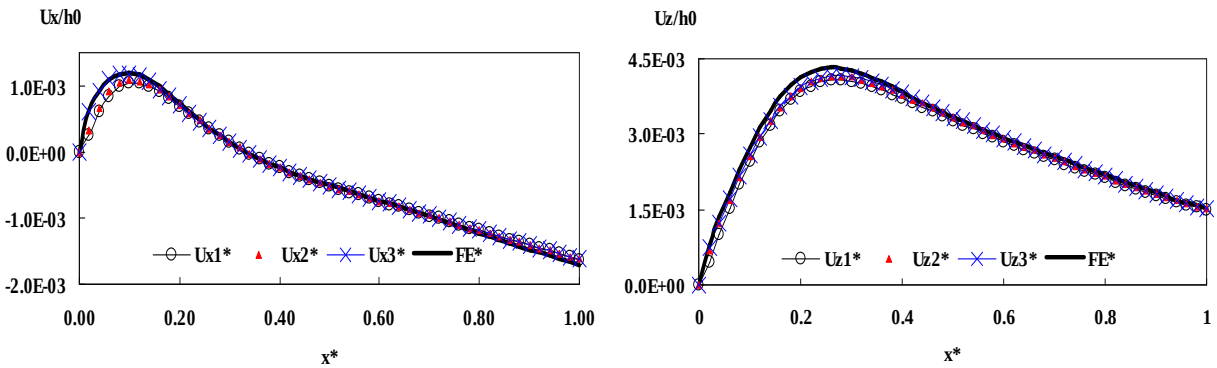

Figure 5. Axial (left) and radial (right) displacement for various approximations. See (11).

the inner wall of the shell. $x^* = x/L$ in the graphs is the vertical position of each point on the inner wall of the shell.

Figure 5 shows that, by using higher-order theories (Uz_2, Uz_3, Ux_2, and Ux_3), the displacements do not change significantly. The maximum percentage of difference between the FE and shear deformation results is 7% for Uz_1, 5% for Uz_2, and 4.8% for Uz_3, which is in agreement with Figure 2, top, for this case study ($3 < m < 4.5$). In Figure 6, it is seen that by using Uz_2 and Uz_3, for the radial displacement,

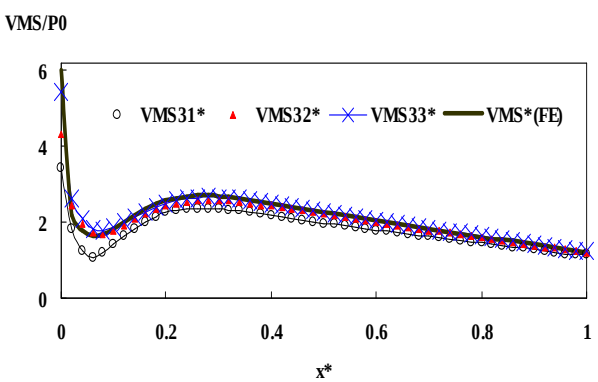

Figure 6. Von Mises stress for different theories. See (11).

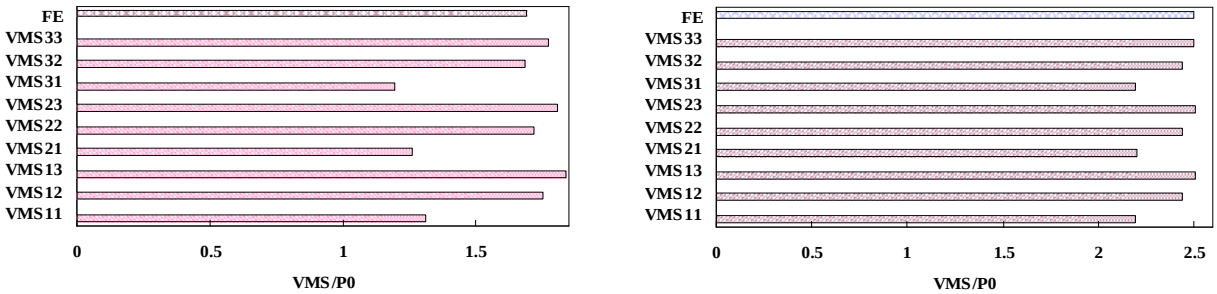

Figure 7. Effect of various theories on von Mises Stress at $x^* = 0.08$ (left) and $x^* = 0.4$ (right).

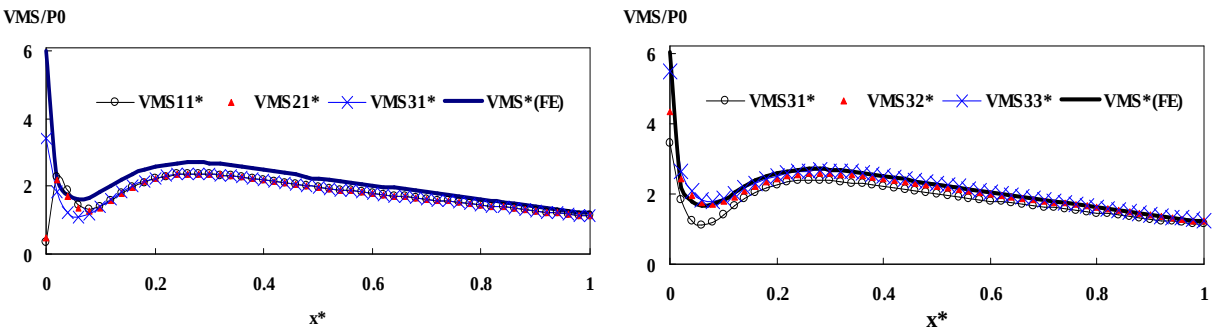

Figure 8. Comparison of different axial displacements for Uz_1 (left) and radial displacements for Ux_3 (right) on von Mises stress.

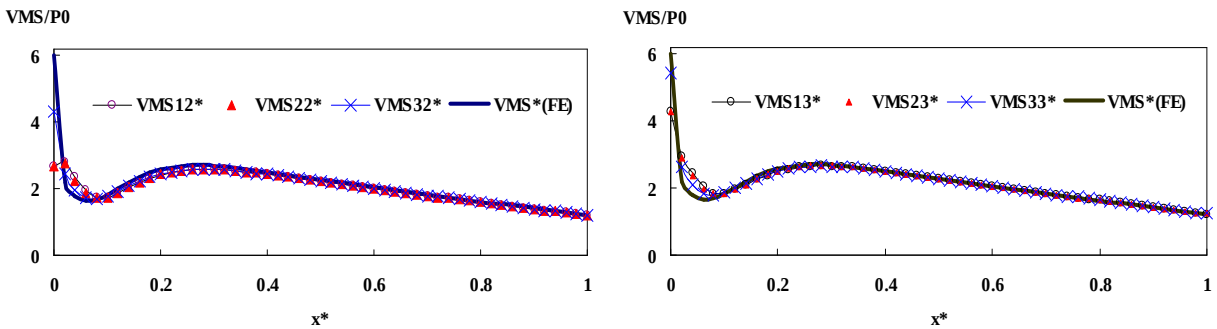

Figure 9. Comparison of different axial displacements on von Mises stress for Uz_2 (left) and Uz_3 (right).

the von Mises stress will improve. This result has been shown in Figure 7 for the point $x^* = 0.08$ (a point on the inner wall, near the boundary, and so related to the inner solution) and at $x^* = 0.4$ (a point away from the boundaries, and so related to the outer solution). Also, the difference between the Uz_2 and Uz_3 approximations is not noticeable on the von Mises stress.

Figure 8, left, compares the von Mises stress for the cases 3, 6 and 9 listed in (11). The higher-order theories in axial displacement (Ux_2 and Ux_3) do not affect the stress distribution except near the boundaries. Figure 9 shows the effect of higher-order radial displacements on the von Mises stress distribution. There is no significant difference between the Uz_2 and Uz_3 solutions but Uz_2 and Uz_3 are

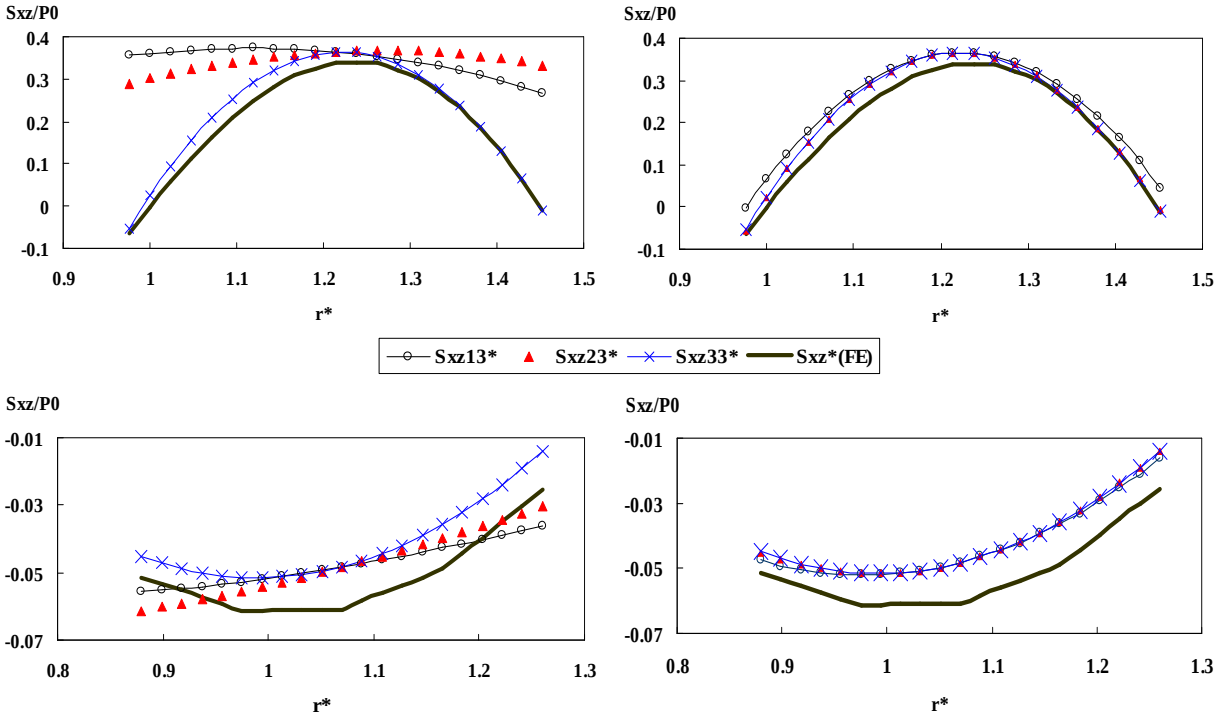

Figure 10. Comparison of different axial displacements on shear stress at $x^* = 0.08$ (top) and $x^* = 0.4$ (bottom), for Uz_3 (left) and for Ux_3 (right).

more accurate than Uz_1 for calculating the von Mises stress. Figure 8, right, suggests that Uz_3 is a very good approximation with respect to the FE results.

Figure 10, top, compares different axial approximations on the shear stress distribution at the section $x^* = 0.08$ in terms of $r^* = r/R_{i0}$ where R_{i0} is the inner radius at $x^* = 0$ (see Table 1). Ux_3 improves the shear stress distribution; the results using Ux_1 and Ux_2 are not suitable. According to Figure 10, right, the higher-order approximations for radial displacement do not change significantly the shear stress distribution at this section. Similar results can be found when one uses Ux_1 or Ux_2 as the axial displacement.

The effect of different theories on the shear stress at section $x^* = 0.4$ is shown in the bottom row of Figure 10. The higher-order approximations are more important for the axial displacement than for the radial displacement in the shear stress distribution at this section.

7. Conclusion

By dividing the solution region into three parts and finding a closed-form solution for each region using the MAE method, it is possible to determine an analytical solution for the governing equations with fast convergence and good accuracy.

The calculations show that the relative difference between the presented results and FE (or elasticity) is not due to the MAE technique but it relates to the selected displacement field.

The results show that FSDT is sufficient for determining the displacements, but that for calculating the von Mises Stress it is necessary to use a higher-order approximation for the radial displacements. The shear stress is small compared to the von Mises stress. The shear stress is sensitive to the selected axial displacement, and Ux_1 and Ux_2 cannot predict its distribution as well, especially at the sections near the boundaries.

As a result, TSDT for the axial and radial displacements is a good approximation for both von Mises and shear stresses; see Equation (1).

References

[Buchanan and Wong 2001] G. R. Buchanan and F. T.-I. Wong, "Frequencies and mode shapes for thick truncated hollow cones", *Int. J. Mech. Sci.* **43**:12 (2001), 2815–2832.

[Correia et al. 2003] I. F. P. Correia, C. M. Mota Soares, C. A. Mota Soares, and J. Herskovits, "Analysis of laminated conical shell structures using higher order models", *Compos. Struct.* **62**:3–4 (2003), 383–390.

[Cui et al. 2001] W. Cui, J. Pei, and W. Zhang, "A simple and accurate solution for calculating stresses in conical shells", *Comput. Struct.* **79**:3 (2001), 265–279.

[Eipakchi et al. 2008] H. R. Eipakchi, S. E. Khadem, and G. H. Rahimi S., "Axisymmetric stress analysis of a thick conical shell with varying thickness under nonuniform internal pressure", *J. Eng. Mech.* (*ASCE*) **134**:8 (2008), 601–610.

[Garg et al. 2006] A. K. Garg, R. K. Khare, and T. Kant, "Free vibration of skew fiber-reinforced composite and sandwich laminates using a shear deformable finite element model", *J. Sandw. Struct. Mater.* **8**:1 (2006), 33–53.

[Nayfeh 1981] A. H. Nayfeh, *Introduction to perturbation techniques*, Wiley, New York, 1981.

[Panferov 1992] I. V. Panferov, "Stresses in a transversely isotropic conical elastic pipe of constant thickness under a thermal load", *J. Appl. Math. Mech.* **56**:3 (1992), 410–415.

[Ramesh et al. 2008] S. S. Ramesh, C. M. Wang, J. N. Reddy, and K. K. Ang, "Computation of stress resultants in plate bending problems using higher-order triangular elements", *Eng. Struct.* **30**:10 (2008), 2687–2706.

[Sivadas and Ganesan 1991] K. R. Sivadas and N. Ganesan, "Vibration analysis of laminated conical shells with variable thickness", *J. Sound Vib.* **148**:3 (1991), 477–491.

[Sundarasivarao and Ganesan 1991] B. S. K. Sundarasivarao and N. Ganesan, "Deformation of varying thickness of conical shells subjected to axisymmetric loading with various end conditions", *Eng. Fract. Mech.* **39**:6 (1991), 1003–1010.

[Tavares 1996] S. A. Tavares, "Thin conical shells with constant thickness and under axisymmetric load", *Comput. Struct.* **60**:6 (1996), 895–921.

[Thambiratnam and Zhuge 1993] D. P. Thambiratnam and Y. Zhuge, "Axisymmetric free vibration analysis of conical shells", *Eng. Struct.* **15**:2 (1993), 83–89.

[Tong 1994] L. Tong, "Free vibration of laminated conical shells including transverse shear deformation", *Int. J. Solids Struct.* **31**:4 (1994), 443–456.

[Wu and Chiu 2002] C.-P. Wu and S.-J. Chiu, "Thermally induced dynamic instability of laminated composite conical shells", *Int. J. Solids Struct.* **39**:11 (2002), 3001–3021.

[Wylie 1979] C. R. Wylie, "Simultaneous linear differential equations", Chapter 5, pp. 147–181 in *Differential equations*, McGraw-Hill, New York, 1979.

Received 21 Nov 2008. Revised 3 Jun 2009. Accepted 3 Aug 2009.

HAMID REZA EIPAKCHI: hamidre_2000@yahoo.com
Mechanical Engineering Faculty, Shahrood University of Technology, P.O. Box 316, Shahrood, Iran